

AD-A081 002

NAVAL RESEARCH LAB WASHINGTON DC

F/O 9/8

MEASURED PERFORMANCE CHARACTERISTICS OF REFLECTIVE BUTLER MATRI--ETC(U)

JAN 80 B SHELEG, H E MEDDINGS

UNCLASSIFIED

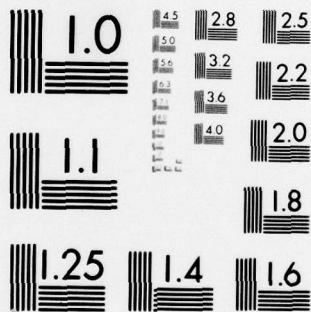
NRL-8361

SDIE-AD-E000 362

NL

OF
AD
A081002





MICROCOPY RESOLUTION TEST CHART
NATIONAL BUREAU OF STANDARDS-1963-A

ADA081002

LEVEL III



ade ooo 362

NRL Report 8361

Measured Performance Characteristics of Reflective Butler Matrices

B. SHELEG AND H. E. HEDDINGS

*Microwave Technology Branch
Electronics Technology Division*

January 9, 1980

DDC FILE COPY



DTIC
ELECTE
FEB 25 1980
S D A

NAVAL RESEARCH LABORATORY
Washington, D.C.

Approved for public release; distribution unlimited.

80 2 1 035

(14) NRL-8361

(9) Final rept.

SECURITY CLASSIFICATION OF THIS PAGE (When Data Entered)

REPORT DOCUMENTATION PAGE		READ INSTRUCTIONS BEFORE COMPLETING FORM
1. REPORT NUMBER NRL Report 8361	2. GOVT ACCESSION NO.	3. RECIPIENT'S CATALOG NUMBER
4. TITLE (and Subtitle) (6) MEASURED PERFORMANCE CHARACTERISTICS OF REFLECTIVE BUTLER MATRICES.	5. TYPE OF REPORT & PERIOD COVERED Final report on one phase of a continuing NRL problem	
7. AUTHOR(s) (10) B. Sheleg and H.E. Heddings	6. PERFORMING ORG. REPORT NUMBER	
9. PERFORMING ORGANIZATION NAME AND ADDRESS Naval Research Laboratory Washington, DC 20375	8. CONTRACT OR GRANT NUMBER(s) (11) 9 Jan 80	
11. CONTROLLING OFFICE NAME AND ADDRESS Department of the Navy Office of Naval Research Arlington, VA 22217	10. PROGRAM ELEMENT, PROJECT, TASK AREA & WORK UNIT NUMBERS NRL Problem R08-63 Program Element 61153N-21 Project RR021-03	
14. MONITORING AGENCY NAME & ADDRESS (if different from Controlling Office) (10) RR02143 (17) RR0210346	12. REPORT DATE January 9, 1980	
	13. NUMBER OF PAGES 31 (12) 32	
	15. SECURITY CLASS. (of this report) UNCLASSIFIED	
	15a. DECLASSIFICATION/DOWNGRADING SCHEDULE	
16. DISTRIBUTION STATEMENT (of this Report) Approved for public release; distribution unlimited. (18) SBIE (19) AD-E000 362		
17. DISTRIBUTION STATEMENT (of the abstract entered in Block 20, if different from Report)		
18. SUPPLEMENTARY NOTES		
19. KEY WORDS (Continue on reverse side if necessary and identify by block number) Antenna feed network Multibeam antenna Printed-circuit techniques		
20. ABSTRACT (Continue on reverse side if necessary and identify by block number) A reflective Butler matrix is described which has the full electrical performance of a conventional Butler matrix while requiring only 1/2 the usual size and number of circuit components and ports. Reflective networks having eight and 16 ports were built, tested, and evaluated at 1060 MHz. Details of the circuit design and fabrication are included. The measured performance characteristics of the reflective Butler matrix are shown to compare well with those of a conventional Butler matrix.		

DD FORM 1 JAN 73 1473

EDITION OF 1 NOV 65 IS OBSOLETE
S/N 0102-014-6601

i SECURITY CLASSIFICATION OF THIS PAGE (When Data Entered)

251950

JOB

CONTENTS

INTRODUCTION	1
PROPERTIES OF A BUTLER MATRIX	1
DESIGN AND FABRICATION	2
TEST AND EVALUATION	3
SUMMARY	3
REFERENCES	3
APPENDIX A — Measured Results for the 16-Port Reflective Butler Matrix	13

Accession For	
NTIS GRA&I	<input checked="checked" type="checkbox"/>
DOC TAB	
Unannounced	
Justification	
By	
Distribution/	
Availability Codes	
Dist.	Avail and/or special
A	

MEASURED PERFORMANCE CHARACTERISTICS OF REFLECTIVE BUTLER MATRICES

INTRODUCTION

The suitability of Butler-matrix feed networks for linear-array and circular-array antenna applications is well documented in the literature [1-6]. However, because Butler matrices rapidly become unwieldy as the input-output ports increase in number, their expected use in feed systems for large arrays has not materialized. This inherent inhibiting characteristic of large conventional Butler matrix circuits is addressed in this effort. A reflective Butler matrix is described which has the full electrical performance of a conventional Butler matrix while requiring only 1/2 the usual size and number of circuit components.

This report represents the experimental part of a cooperative effort on multibeam antenna research. The design, fabrication, testing, and evaluation of a 16-port reflective Butler matrix is presented. The theoretical portion of this work was previously reported by Shelton and Hsiao [1].

PROPERTIES OF A BUTLER MATRIX

A Butler matrix is a lossless, passive network having N inputs and N outputs, where N usually is some power of 2. The inputs are matched and isolated from one another, as are the outputs. A signal into any input results in currents of equal amplitude on all the outputs with phase varying linearly across the outputs. Each input port has a unique output linear phase progression associated with it. Hence, if the outputs are connected properly to any array of N radiators, N different antenna aperture current distributions can be realized by using different input ports.

Butler-matrix networks have essentially two circuital components: phase shifters and 3-dB hybrid couplers. Although a variety of 3-dB hybrids can be used in these circuits, only the 3-dB phase-quadrature directional coupler shall be considered here. For a $2N$ -port Butler matrix, where $N = 2^n$, the total number of hybrids is $n2^{n-1}$, which clearly shows the growth relationship between the array size and its corresponding Butler matrix feed. In practice it is rare to find Butler matrices with more than 64 output ports, because dimensional tolerances become too stringent. A technique has been developed which symmetrizes Butler matrices along a line midway between the input and output ports. This network, somewhat analogous to a lens system, can be "reflected" along this line of symmetry and remain fully functional. A signal into any input will travel forward to the line of symmetry and becomes reflected back to the input ports which now assume the role of "output ports." This network is called a reflected Butler matrix, and the details of its design, testing, and performance follow.

Manuscript submitted September 14, 1979.

DESIGN AND FABRICATION

Symmetrized Butler-matrix networks fall into two classes depending on whether n is odd or even in the expression for the number of ports $N = 2^n$. The value of n specifies the number of rows of hybrids between the input and output ports in a conventional Butler matrix. Since the network "cutting" is along the line of symmetry of the matrix, it follows that for $n = 2, 4, 6, \dots$ the cut will fall between two rows of hybrids but for $n = 1, 3, 5, \dots$ the cut falls directly on the center row of hybrids. Both cases shall be considered.

An eight-port conventional Butler matrix is shown in Fig. 1. The 12 couplers in this network are arranged equally in three rows ($n = 3$) of $N/2$ hybrids. When this matrix is cut or folded as shown in Fig. 2, some hybrids must be cut in half. A 3-dB coupler consisting of two 8.3-dB directional couplers connected in tandem was selected as the simplest way of making a half coupler. The folded 3-dB quadrature hybrid coupler is obtained simply by placing open terminations on the through and coupled arms of an 8.3-dB directional coupler, as shown in Fig. 3. Care must be taken to position both open terminations the same distance from the coupling region; the absolute distance is irrelevant. The measured performance of this half hybrid compares quite well with that of a conventional hybrid made up of two 8.3-dB couplers connected in tandem (Figs. 4 and 5). In this effort there was no attempt to achieve broadband performance; thus the hybrids used a single $1/4$ -wavelength coupling section.

The folded eight-port Butler matrix shown in Fig. 6 was designed for midband frequency of 1060 MHz and was fabricated in printed-circuit shielded-stripline media. Three sandwiched sheets of 1.6-mm (1/16 in.) Duroid was used to fabricate the circuit, with the center board having etched circuits on both sides. This construction permits broadside coupling of the lines and minimizes the problem of transmission-line crossover in the network layout. A detailed engineering drawing of this circuit appears in Fig. 7.

The 16-port reflective Butler matrix, shown in Fig. 8, represents the class of networks having n equal to an even integer. For this case of $n = 4$, there would be four rows of hybrids, and each row would have eight hybrids for a network total of 32 couplers. The line of symmetry for this network lies midway between two rows of hybrids, and the network "cutting" involves only transmission lines. The layout of this complex circuit was done on an in-house graphic-display computer-aided digitizing network. All corrections and modifications to the matrix circuit are conveniently accomplished via magnetic tape. This method eliminates the human error and the long turnaround times encountered when drawings must be redrawn by hand. Once the desired reflective network design is achieved, a mask is made by using an Electro-Mask Pattern Generator. This is an optical exposure system which produces 127-mm-by-127-mm (5-by-5-in.) masks on glass plates. The mask of the 16-port reflective matrix is shown in Fig. 9. It was necessary to enlarge these masks by a factor of 5 to gain the required size of the negative or mask. The fabrication of the 16-port network was the same as that used for the eight-port folded Butler matrix, with the major difference being the metal cover plates and rivets used to bond the circuit boards together.

TEST AND EVALUATION

Special attention is required during the testing of the reflective Butler matrix, primarily because the through signal becomes reflected and is mixed at the input/output port with other return signals due to network and port termination mismatches. *Uniformly* well matched loads on the ports of this matrix network are a requirement for good measurements and accurate performance evaluation.

An automatic network analyzer (Hewlett-Packard 8545A) was used to test the folded networks. All ports underwent comprehensive testing over the frequency band of 1000 to 1100 MHz. At each test point the phases and amplitudes of the signal input and the return (reflected signal) were measured. Typical measured performance curves of the eight-port and 16-port reflective networks are shown in Figs. 10 and 11 respectively. These measurements were made with all ports terminated in 50-ohm resistive matched loads. The completed set of measured results for the 16-port reflective network appears in the Appendix, with Fig. 11 being the same as Fig. A13. In most cases the measured data curves were translated for the convenience of the reader. This translation amounts to no more than changing the phase of the input signal. Finally in Fig. 12 an attempt is made to give some insight as to the bandwidth performance of these reflective networks. A signal was put into port 4R (which is port 4, as tabulated in Fig. 8), and the output signals were measured for frequencies from 500 to 2000 MHz in increments of 100 MHz. The plotted results show surprisingly that the network remains functional over the entire test bandwidth.

SUMMARY

It has been shown that reflective Butler-matrix networks can be designed and fabricated to provide the same electrical performance as conventional Butler matrices. This includes broadbanding, power handling, and insertion loss. Network cutting (or folding) techniques are described in detail, including the halving of 3-dB hybrid couplers. The overall physical size and number of circuit components of these folded networks is essentially 1/2 that of the conventional networks. However, the penalty for this size reduction is that each port must function as both an input and an output port. Therefore some applications might require output circuit configurations such as switching between ports or placing circulators on each port.

REFERENCES

1. J.P. Shelton and J.K. Hsiao, "Reflective Butler Matrices," NRL Report 8188, Mar. 1978.
2. B. Sheleg, "A Matrix-Fed Circular Array for Continuous Scanning," Proc. IEEE, Special Issue on Electronic Scanning, 56, 2016-2027 (Nov. 1968).
3. J.P. Shelton, "Fast Fourier Transforms and Butler Matrices," Proc. IEEE 56 (No. 3), 350 (Mar. 1968).
4. B. Sheleg, "A Matrix-Fed Circular Array for Continuous Scanning," NRL Report 6696, Apr. 1968.

SHELEG AND HEDDINGS

5. B. Sheleg, "Butler Submatrix Feed Systems for Antenna Arrays," IEEE Trans. Antennas Propagat. AP-21 (No. 2), 228-229, (Mar. 1973).
6. H.J. Moody, "The Systematic Design of the Butler Matrix," Trans. IEEE AP-12 (No. 6.), 786-788 (Nov. 1964).

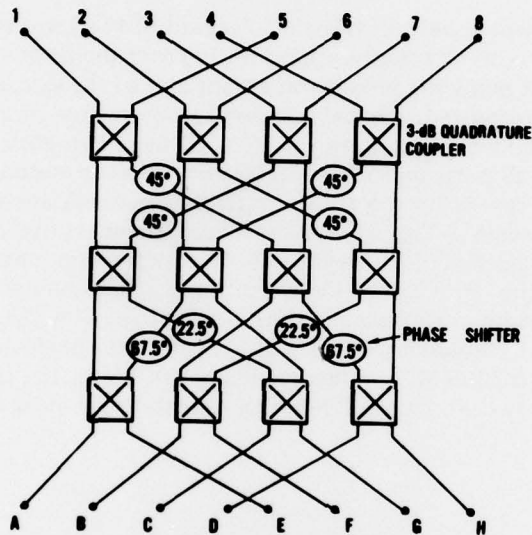


Fig. 1 — Conventional Butler matrix having eight input ports and eight output ports

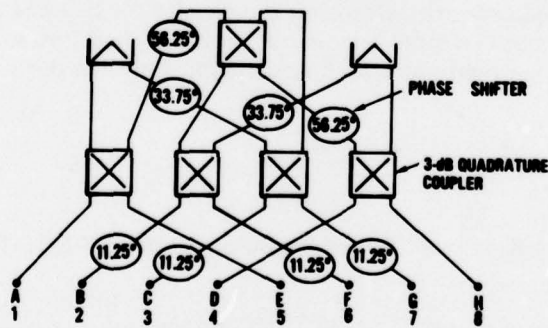


Fig. 2 — Reflective Butler matrix having eight input/output ports

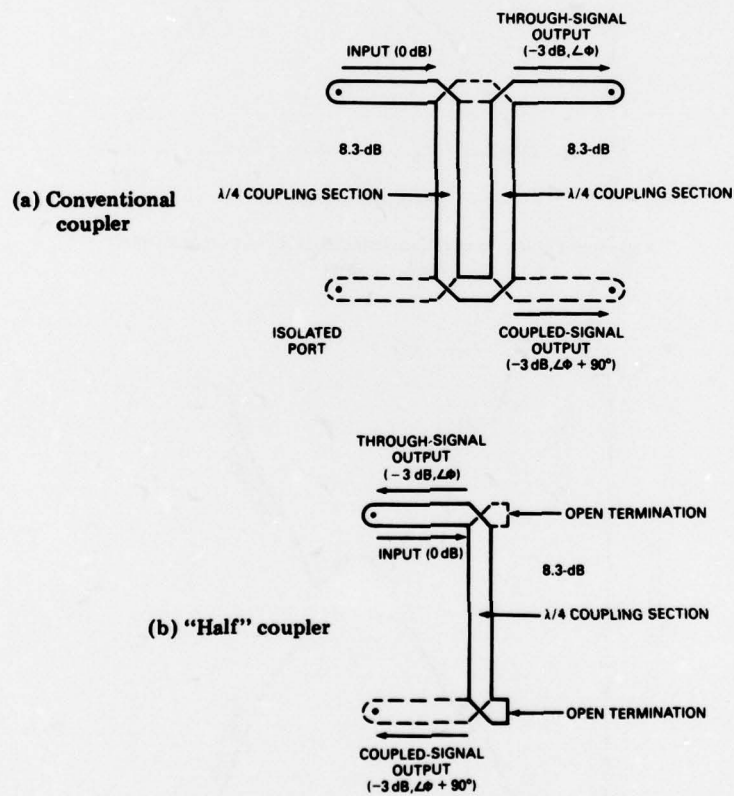


Fig. 3 — Technique for "halving" a 3-dB coupler

SHELEG AND HEDDINGS

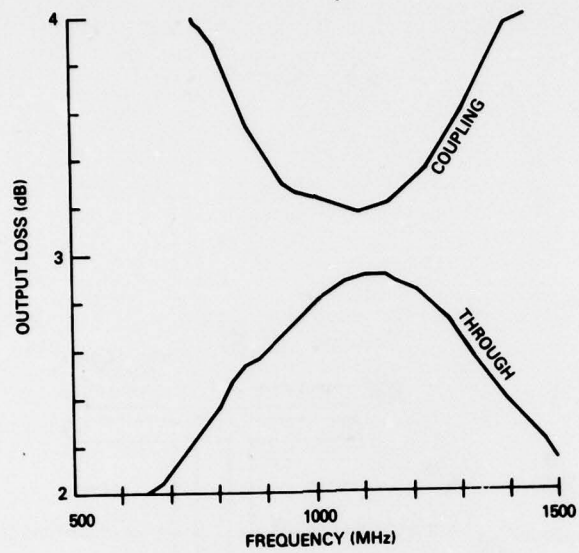


Fig. 4 — Performance characteristics of a conventional 3-dB coupler

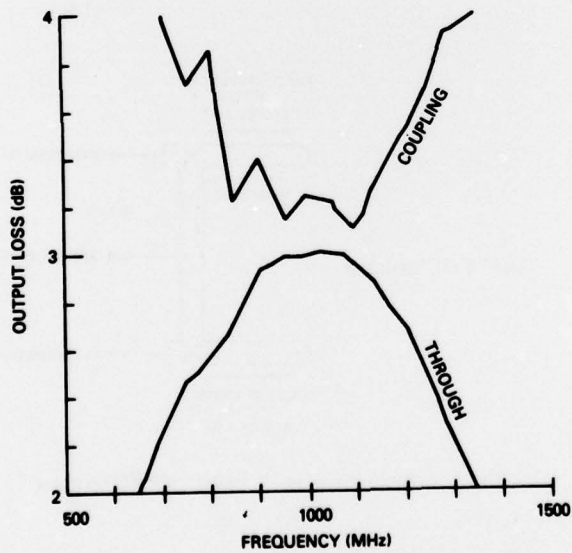
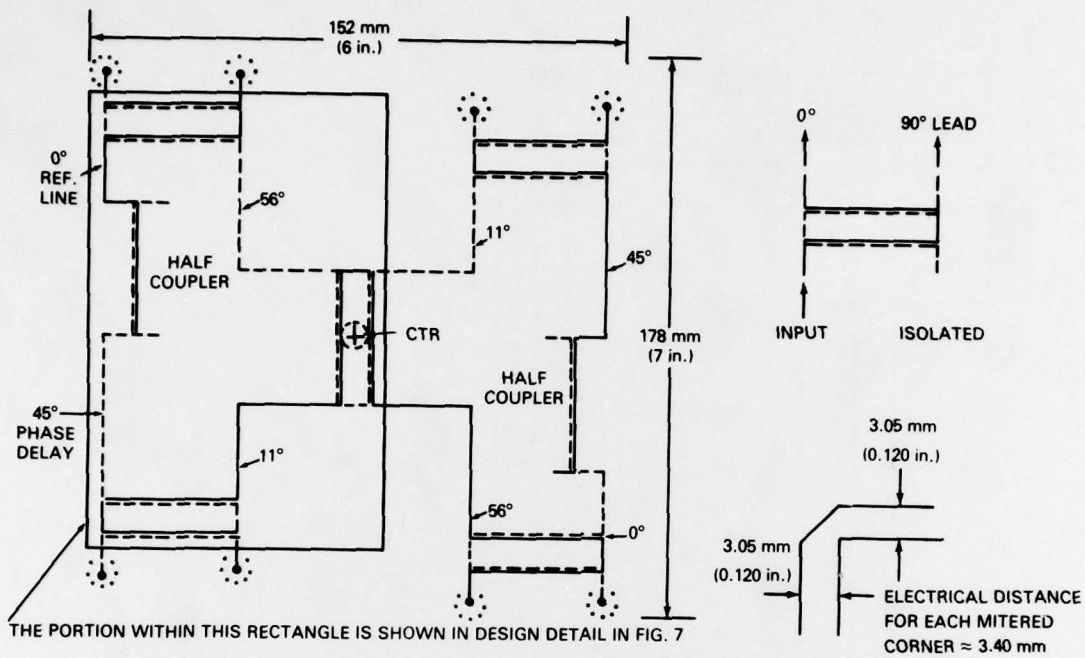


Fig. 5 — Performance characteristics of a half 3-dB coupler

NRL REPORT 8361



THE LAYOUT AS DRAWN ABOVE IS REDRAWN BELOW WITH

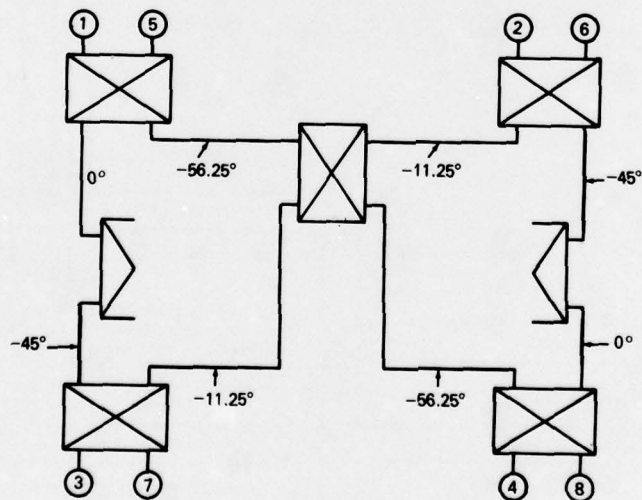
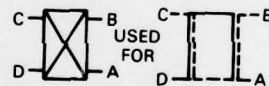


Fig. 6 — Network layout for an eight-port reflective matrix

SHELEG AND HEDDINGS

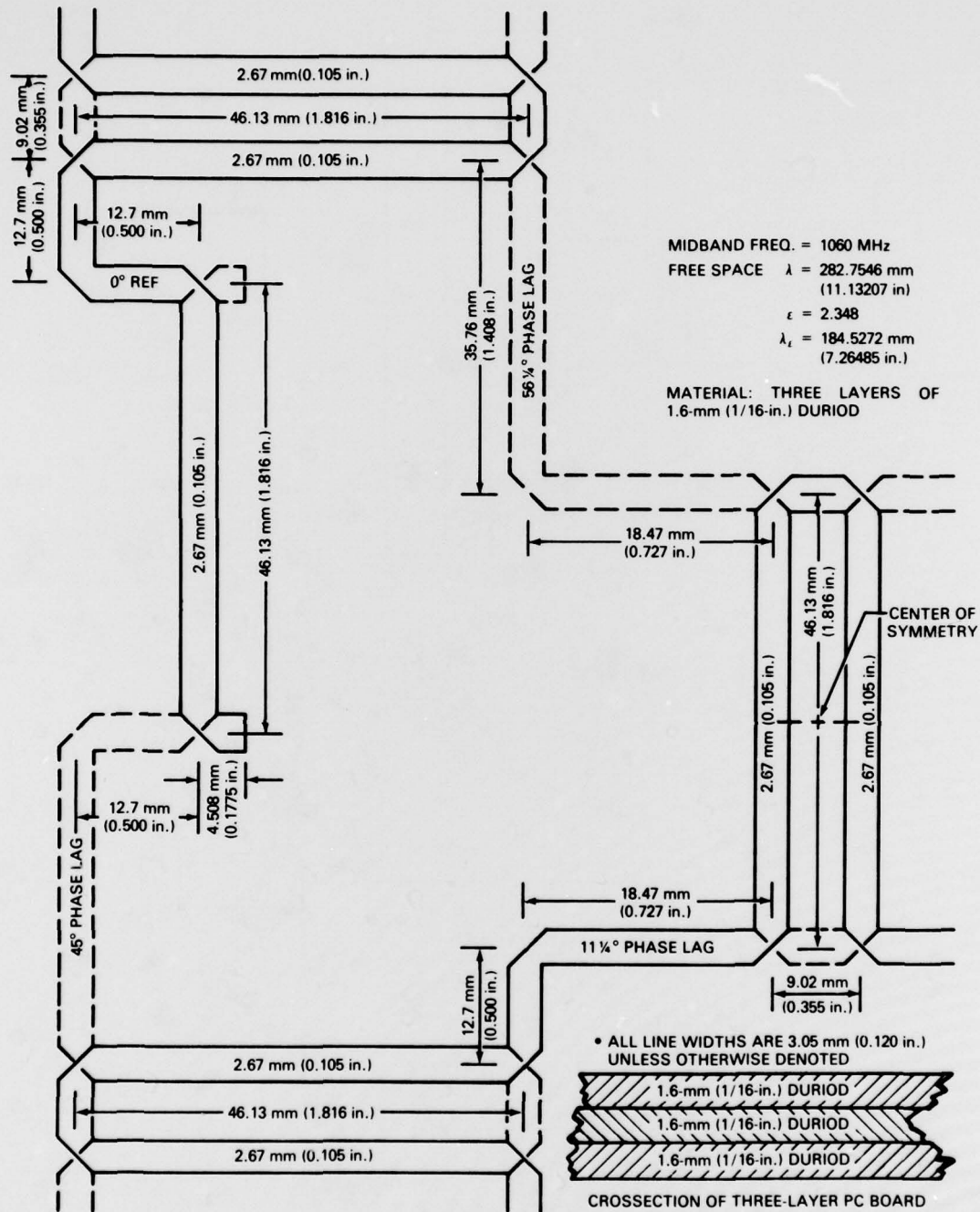


Fig. 7 — Engineering drawing of an eight-port reflective matrix (showing the portion within the rectangle in Fig. 6)

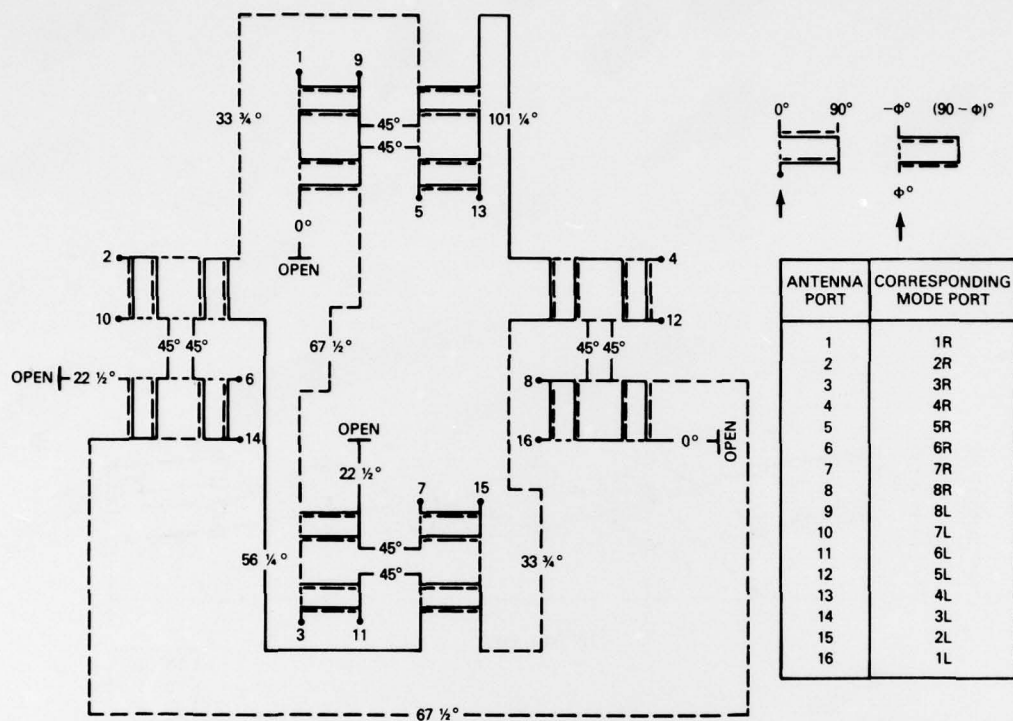


Fig. 8 — Network layout for a 16-port reflective matrix (Fig. 7 shows component dimensions)

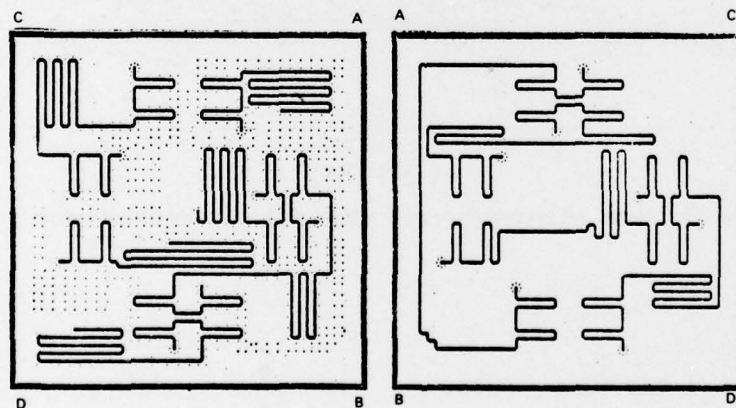


Fig. 9 — Computer-drawn glass-plate masks of the 16-port folded Butler matrix

SHELEG AND HEDDINGS

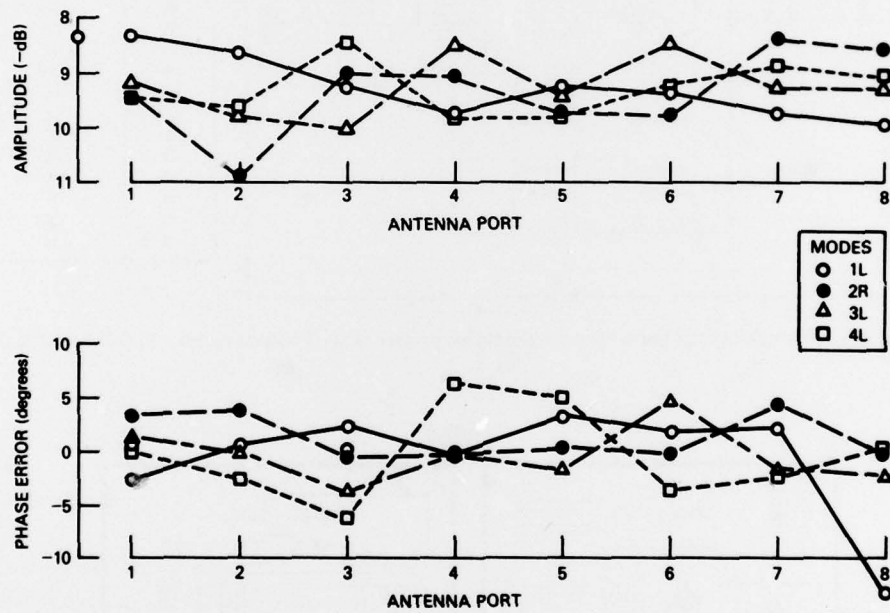


Fig. 10 — Measured performance of the eight-port reflective Butler matrix

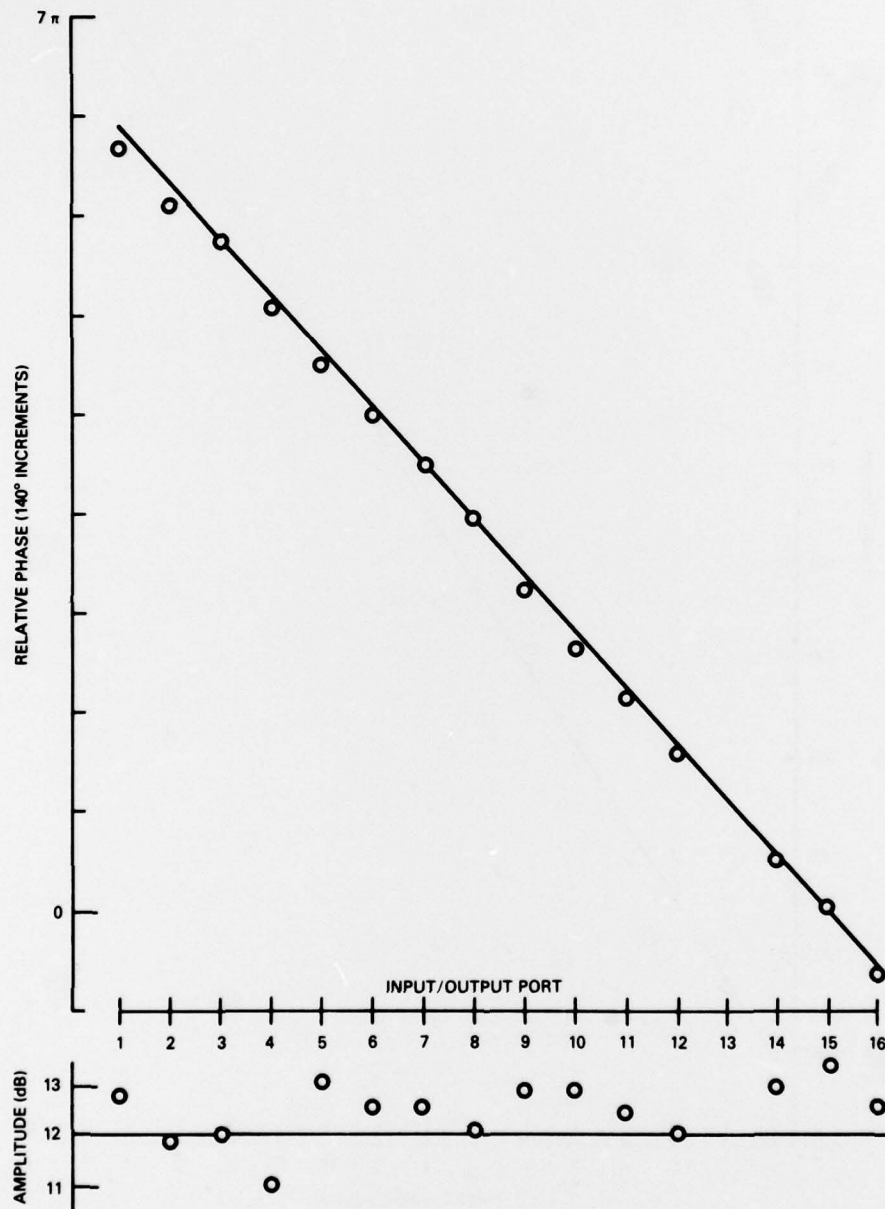


Fig. 11 — Typical measured performance of the 16-port reflective Butler matrix (the Appendix shows the complete test data)

SHELEG AND HEDDINGS

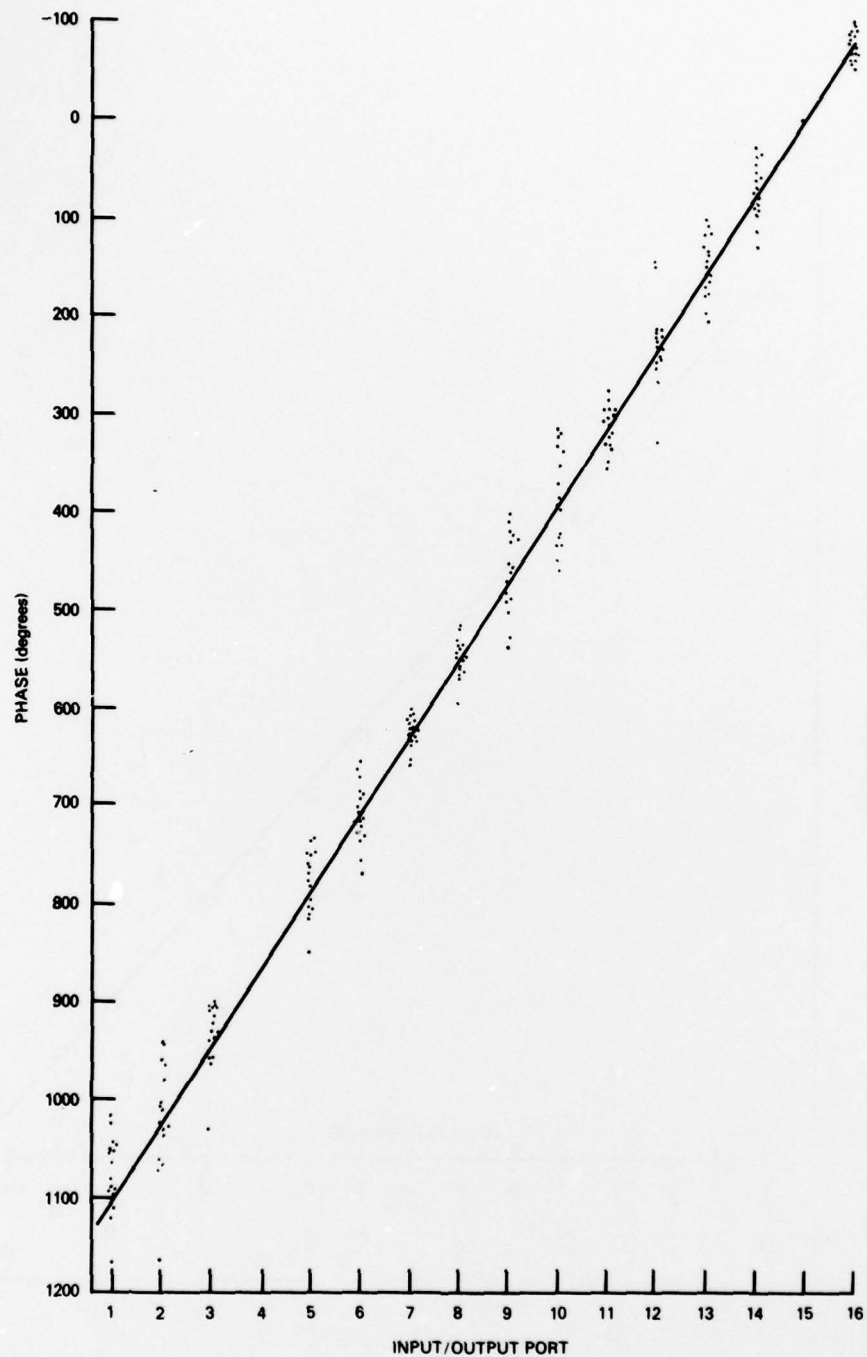


Fig. 12 — Bandwidth performance (500 to 2000 MHz) of port 4 (4R) of the 16-port reflective matrix

Appendix A

MEASURED RESULTS FOR THE 16-PORT REFLECTIVE BUTLER MATRIX

The complete set of measured data for the 16-port reflective Butler matrix is presented in this appendix. The tests were performed using a Hewlett-Packard 8545 automatic network analyzer. All of the phase results were normalized relative to port 15 (in 0° reference) and are shown graphically in Figs. A1 through A16. The amplitude measurements are presented in Table A1 with all values compensated for about 0.5-dB path-insertion loss.

Table A1 — Measured Power Distribution Across the
Output Ports for Different Input Ports

Input Port	Loss in Each Output Port for a Midband Frequency of 1060 MHz (dB)															
	1	2	3	4	5	6	7	8	9	10	11	12	13	14	15	16
1	—	12.1	11.8	12.8	12.0	12.9	12.7	13.2	11.6	12.4	12.6	13.1	12.0	13.0	13.1	12.1
2	11.8	—	12.6	13.1	12.4	13.4	12.8	13.5	11.3	12.2	11.8	12.7	11.8	12.1	12.8	13.3
3	11.8	12.7	—	13.0	11.0	12.0	11.6	12.5	12.4	13.2	13.3	13.7	12.1	13.6	12.5	13.3
4	12.8	13.0	12.9	—	12.2	12.5	12.4	13.0	12.0	12.3	12.5	12.6	10.8	11.8	11.9	13.0
5	12.0	12.5	10.9	12.2	—	13.0	12.0	12.3	12.6	13.1	12.2	13.4	12.9	13.5	12.5	13.0
6	12.8	13.4	12.0	12.7	13.2	—	12.5	13.0	11.9	12.0	10.5	12.0	12.7	13.3	12.3	13.0
7	13.0	13.1	12.0	12.8	12.1	12.7	—	12.1	13.0	13.4	13.1	13.1	12.7	13.0	12.3	12.6
8	13.4	13.6	12.6	13.0	12.5	13.1	12.1	—	13.2	13.0	12.2	13.0	12.3	12.6	11.7	11.9
9	11.7	11.4	12.7	12.2	13.0	12.3	13.3	13.0	—	11.9	13.2	12.5	13.4	11.9	14.2	13.2
10	12.8	12.4	13.5	12.7	13.3	12.5	13.4	13.0	12.0	—	12.8	12.1	12.7	12.0	13.5	12.6
11	12.4	11.9	13.7	13.5	12.1	10.6	12.8	12.8	13.3	13.0	—	13.3	12.7	11.7	13.2	12.9
12	13.1	12.6	13.7	12.7	13.7	12.2	13.1	12.6	12.4	12.0	13.1	—	12.2	11.6	12.5	12.1
13	12.8	11.9	12.0	11.0	18.2	12.6	12.6	12.1	12.9	12.9	12.4	12.0	—	12.9	13.4	12.6
14	12.9	12.2	13.7	12.0	13.5	13.0	13.0	12.4	12.1	12.2	11.7	11.5	12.4	—	12.5	12.0
15	13.2	13.1	12.4	12.0	12.0	12.3	12.3	11.7	14.2	13.6	13.3	12.5	13.3	12.5	—	12.1
16	13.2	13.3	13.5	13.0	13.2	12.8	12.7	11.8	13.0	12.6	12.9	12.1	12.7	12.1	12.1	—

SHELEG AND HEDDINGS

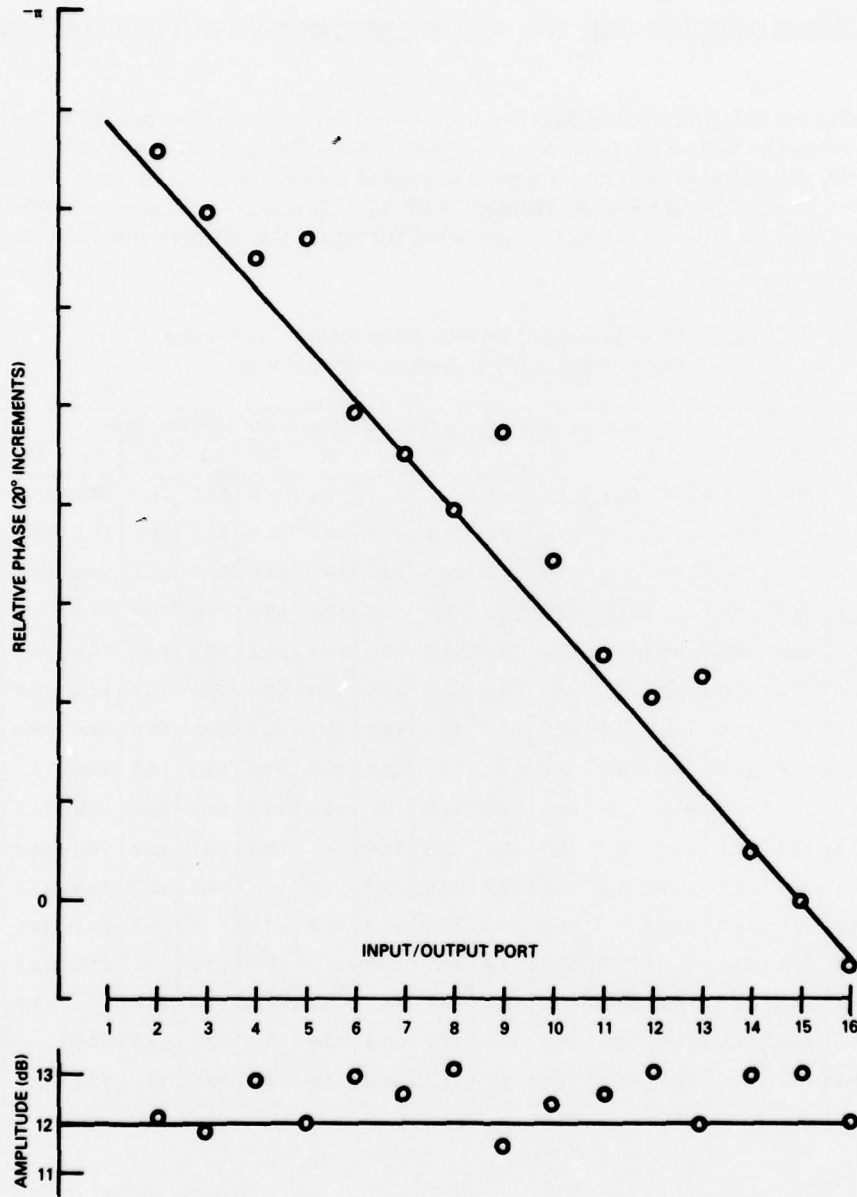


Fig. A1 — Input signal into port 1 (1R)

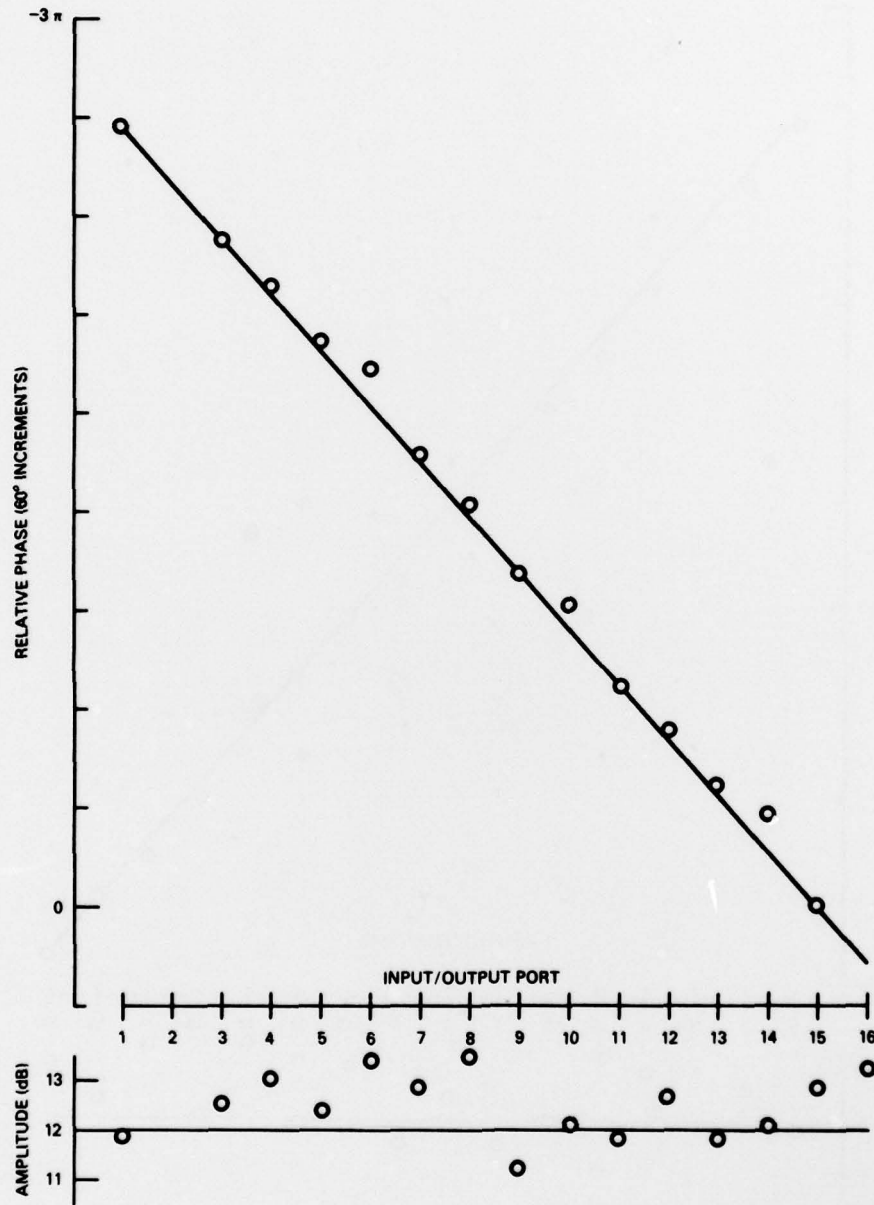


Fig. A2 — Input signal into port 2 (2R)

SHELEG AND HEDDINGS

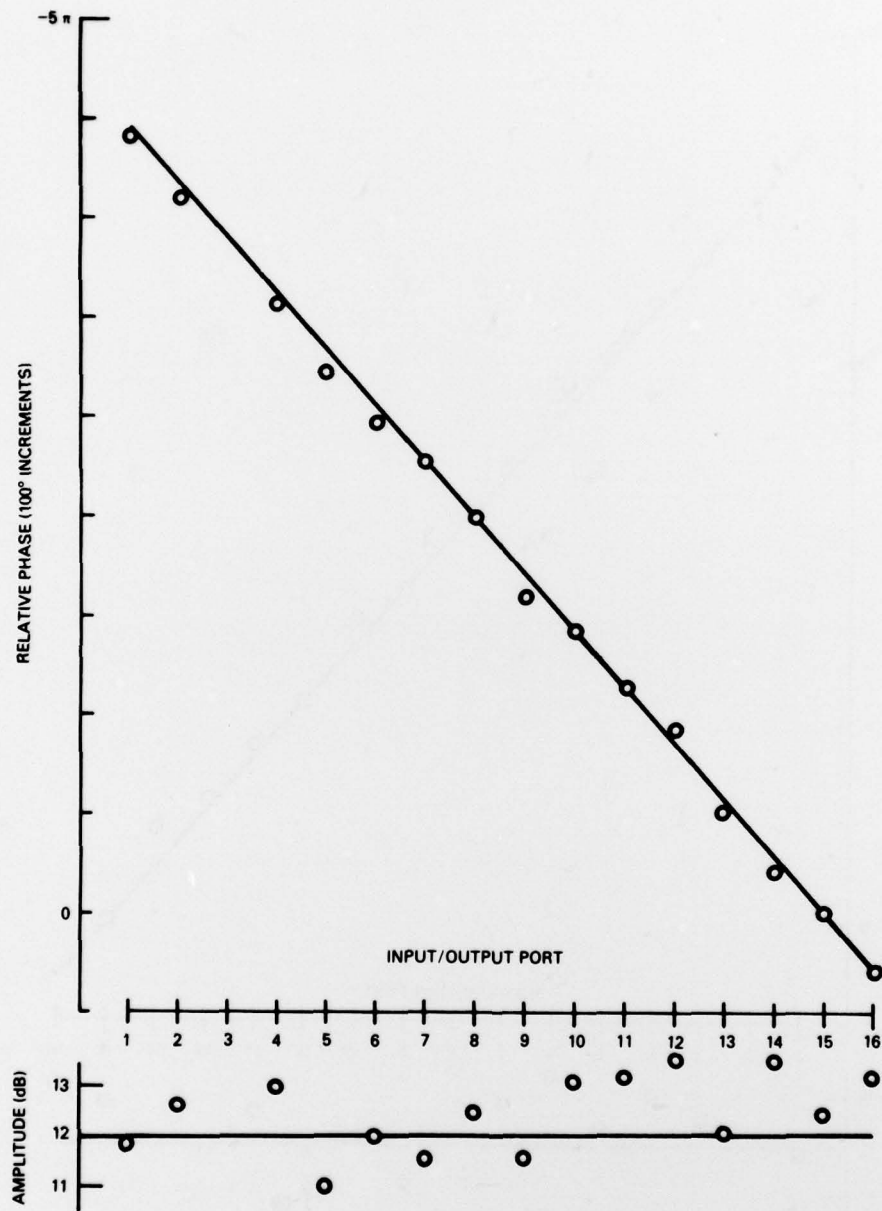


Fig. A3 — Input signal into port 3 (3R)

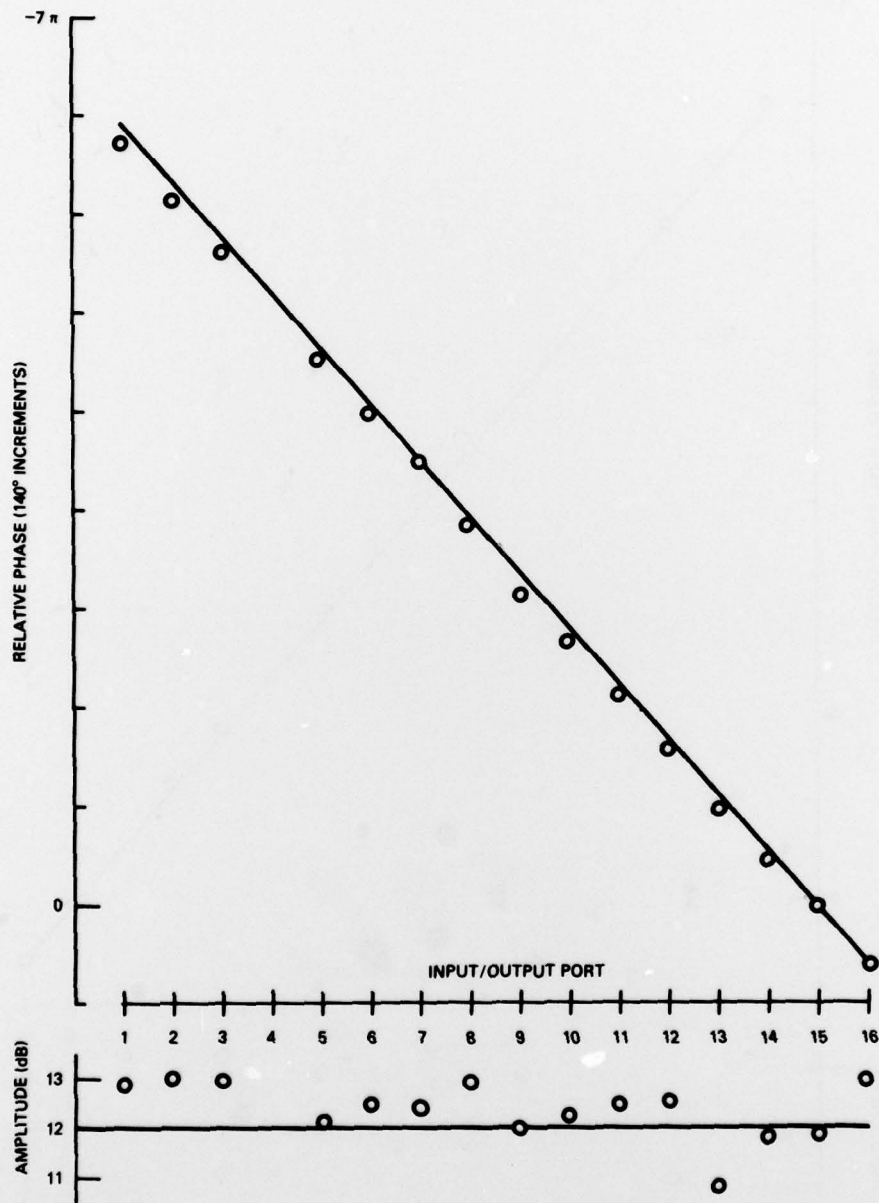


Fig. A4 — Input signal into port 4 (4R)

SHELEG AND HEDDINGS

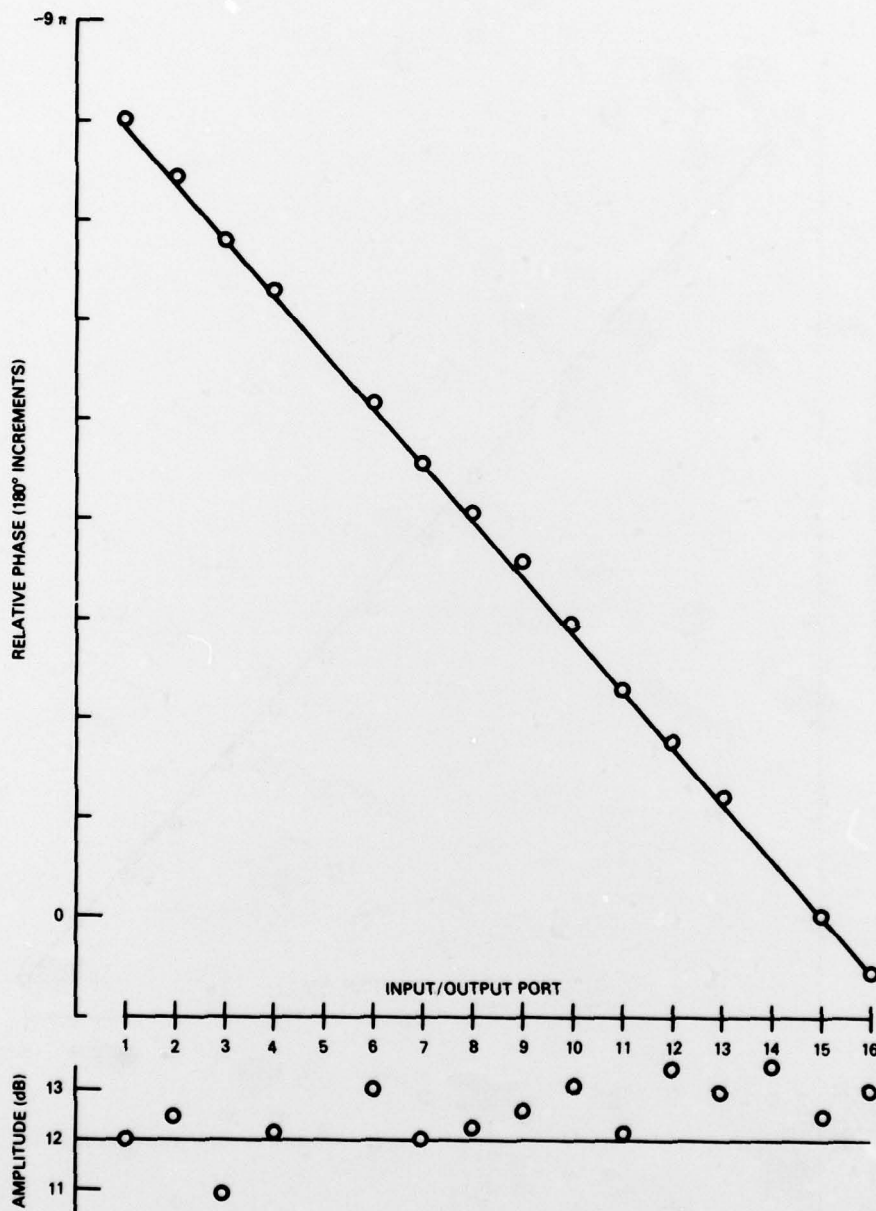


Fig. A5 — Input signal into port 5 (5R)

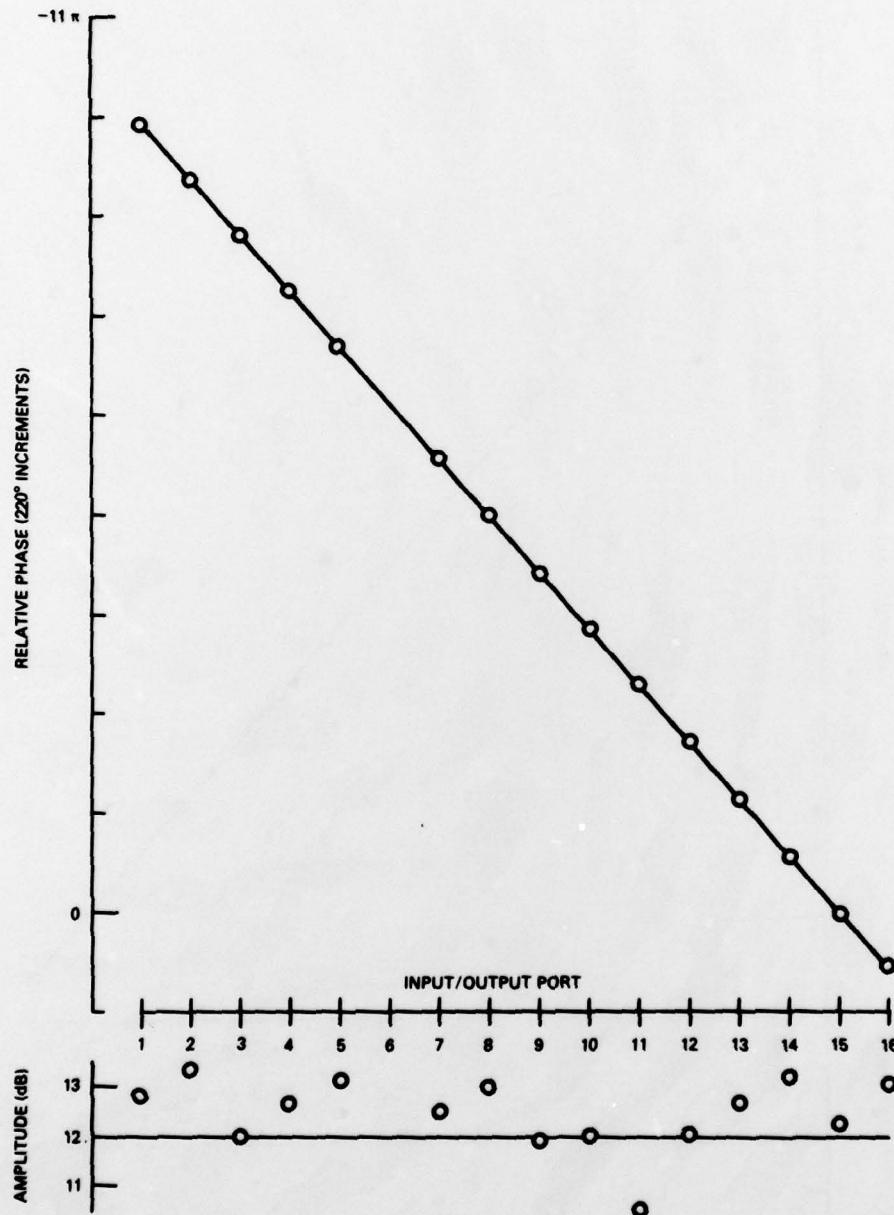


Fig. A6 — Input signal into port 6 (6R)

SHELEG AND HEDDINGS

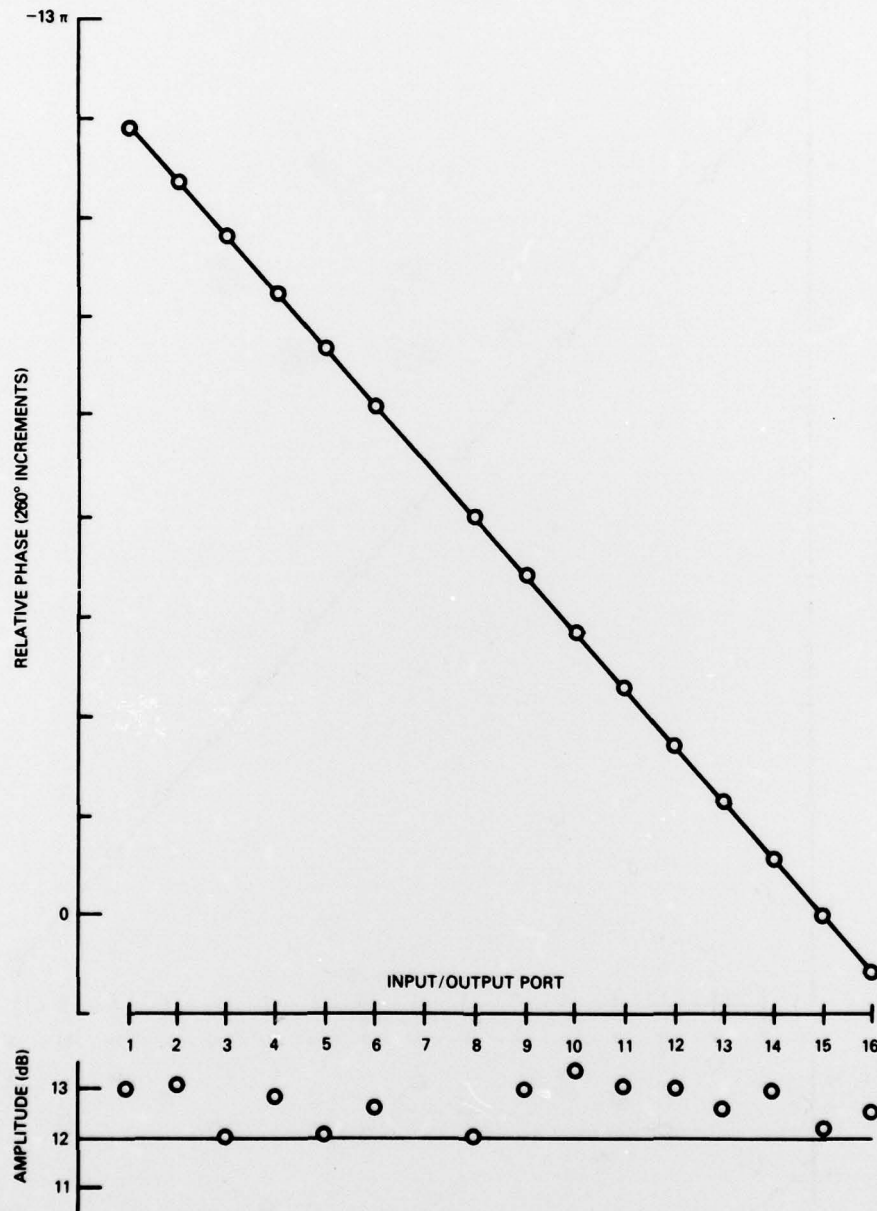


Fig. A7 — Input signal into port 7 (7R)

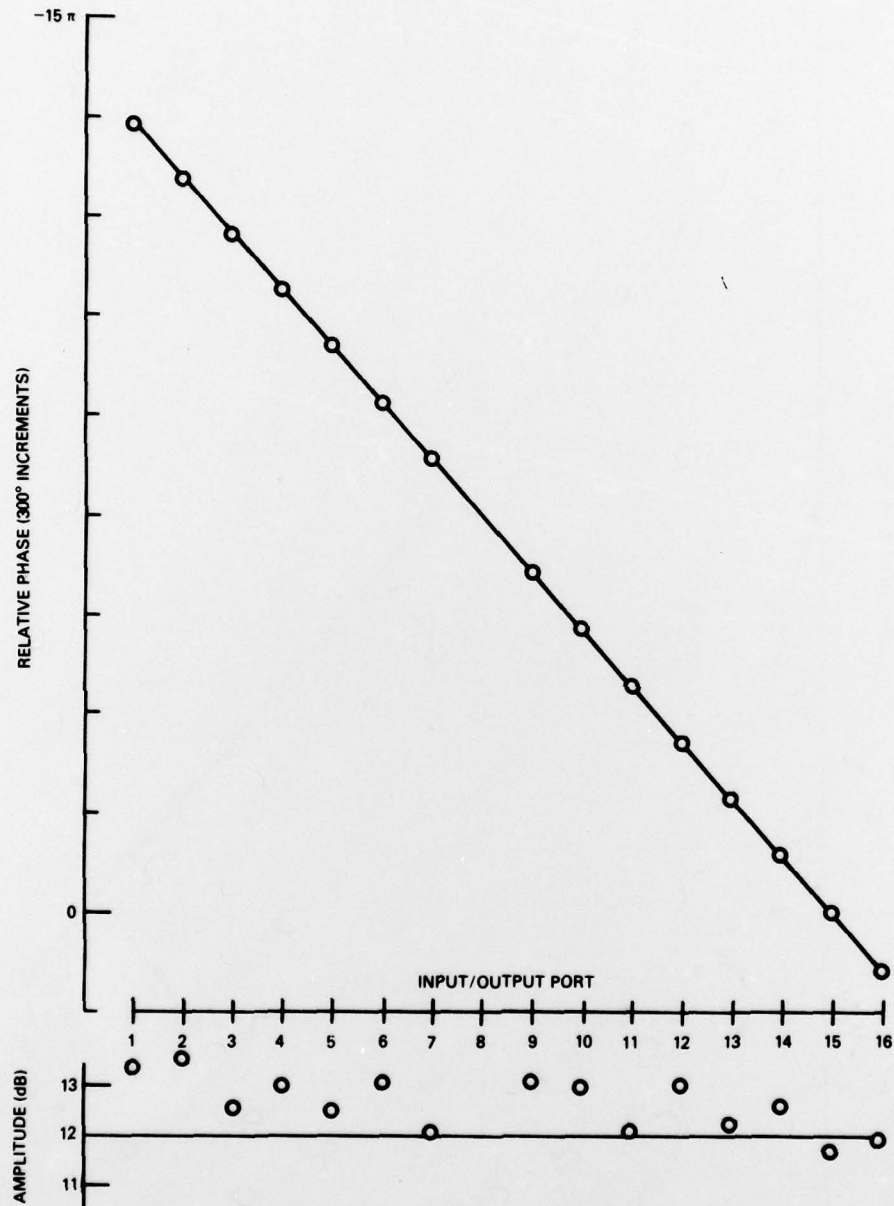


Fig. A8 — Input signal into port 8 (8R)

SHELEG AND HEDDINGS

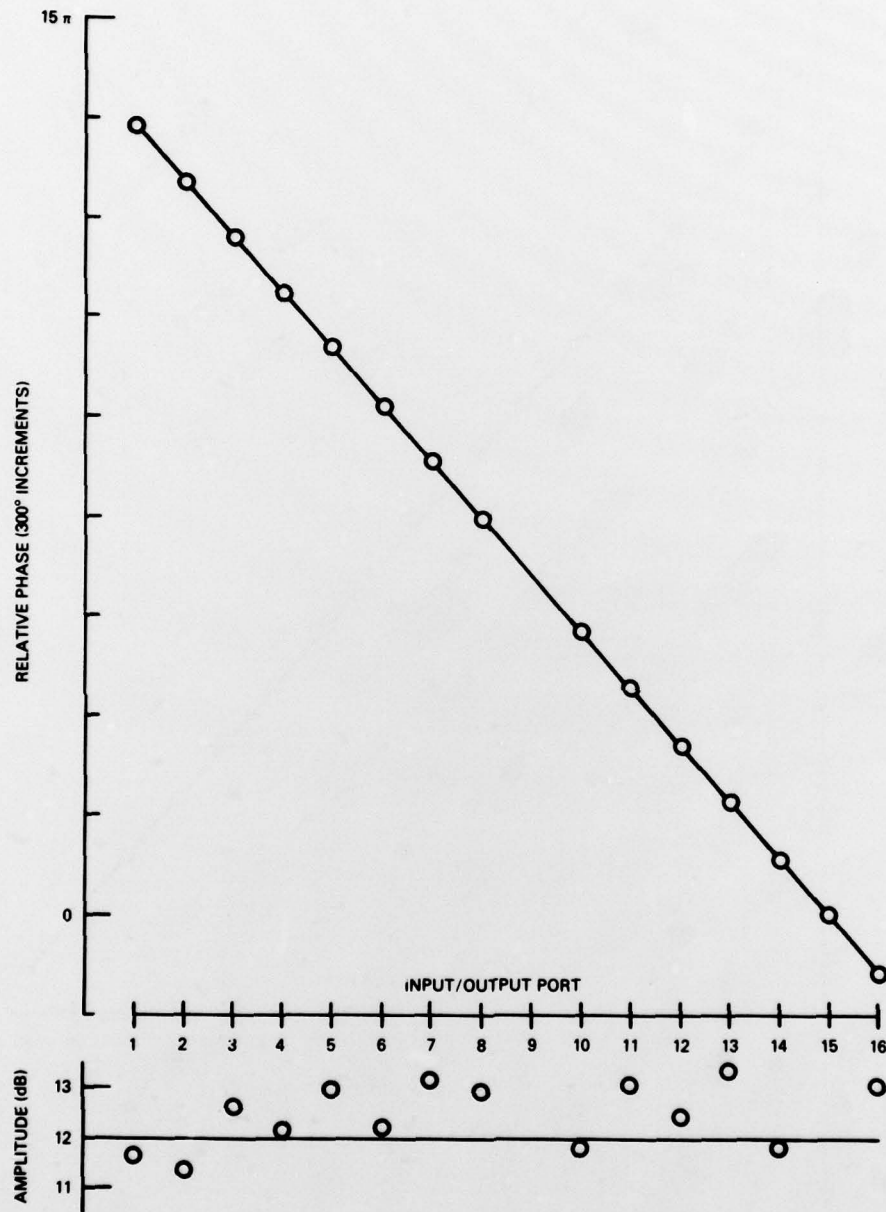


Fig. A9 — Input signal into port (8L)

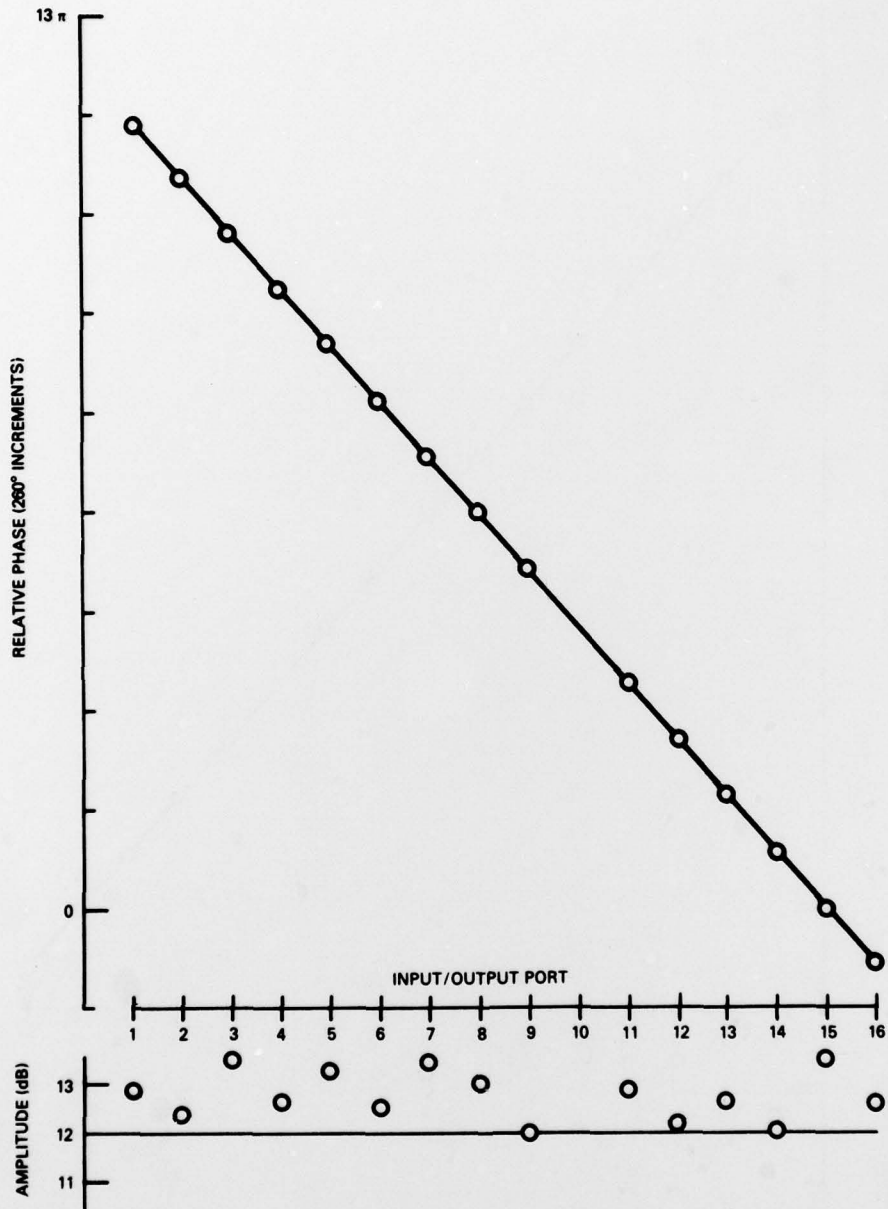


Fig. A10 — Input signal into port 10 (7L)

SHELEG AND HEDDINGS

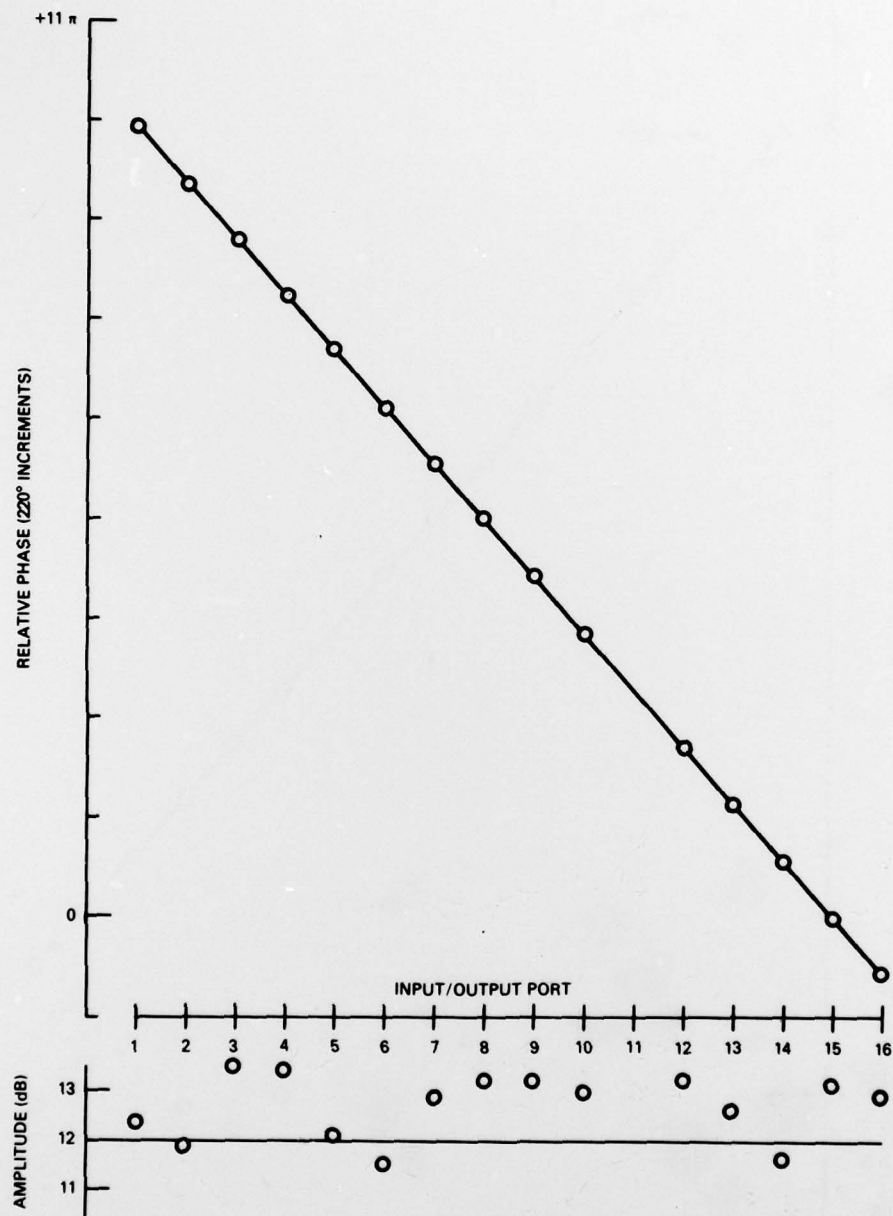


Fig. A11 — Input signal into port 11 (6L)

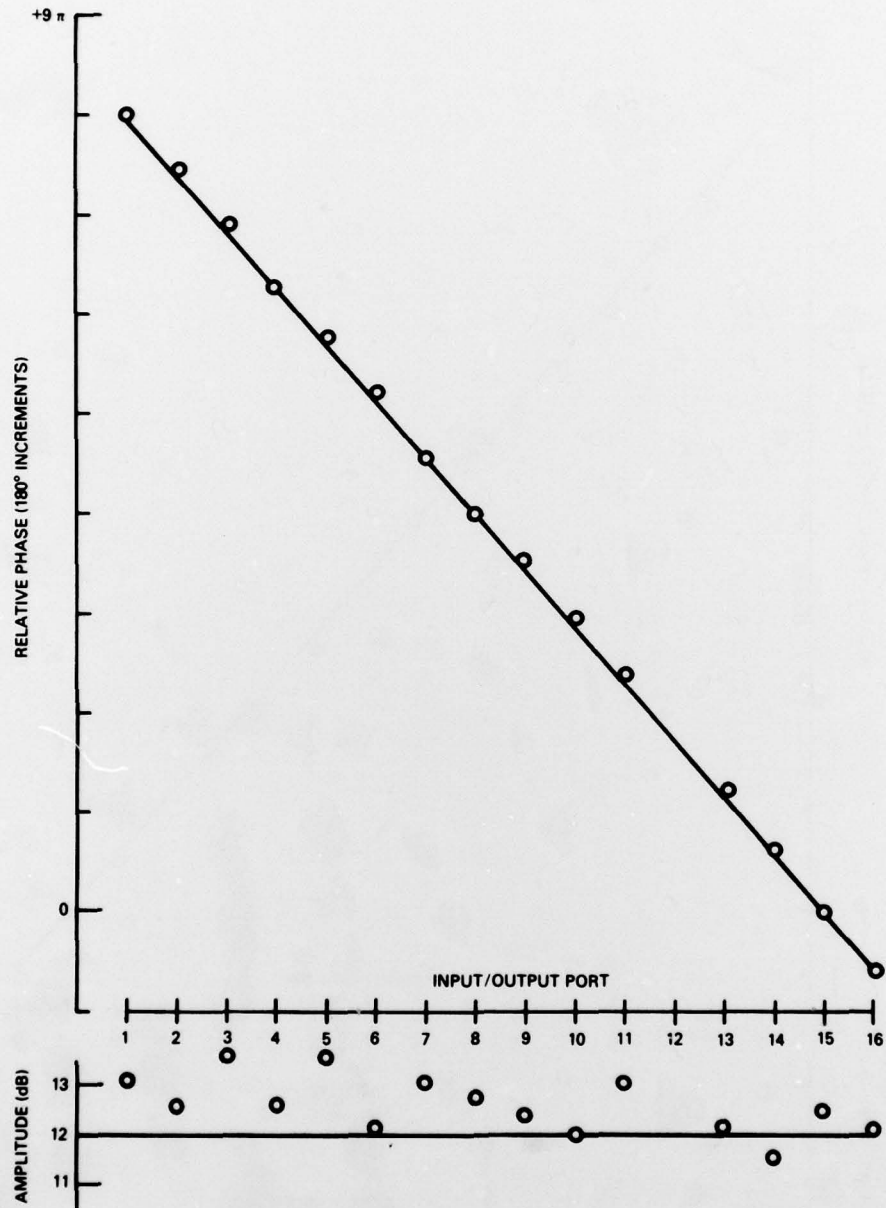


Fig. A12 — Input signal into port 12 (5L)

SHELEG AND HEDDINGS

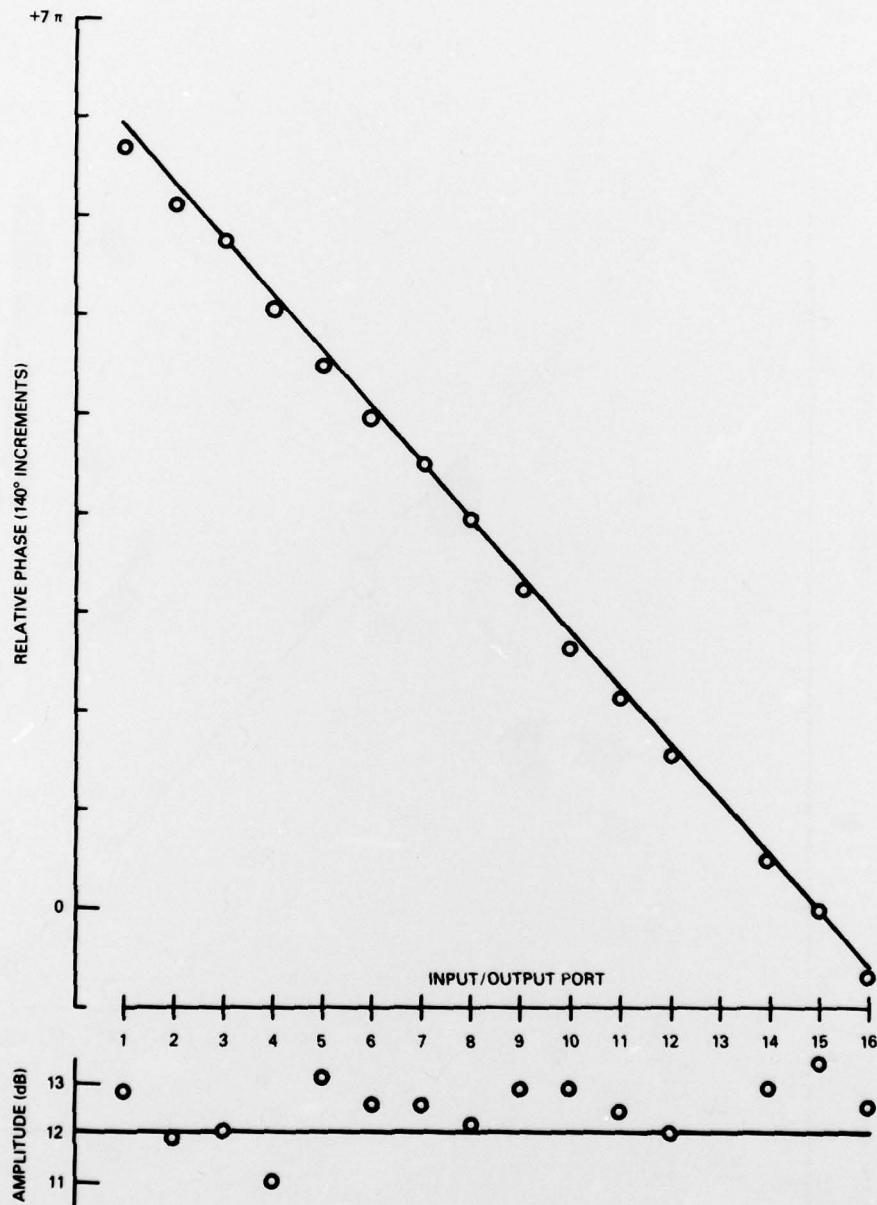


Fig. A13 — Input signal into port 13 (4L)

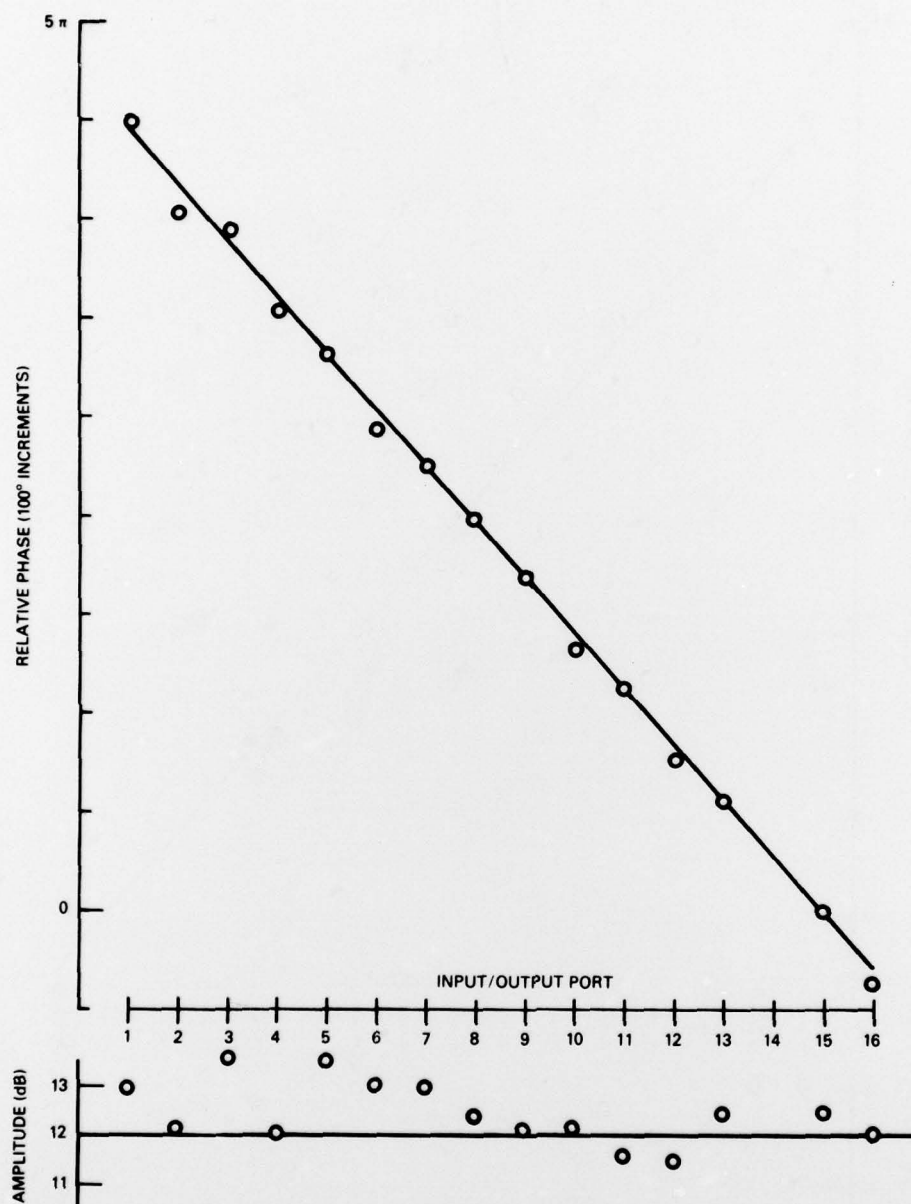


Fig. A14 — Input signal into port 14 (3L)

SHELEG AND HEDDINGS

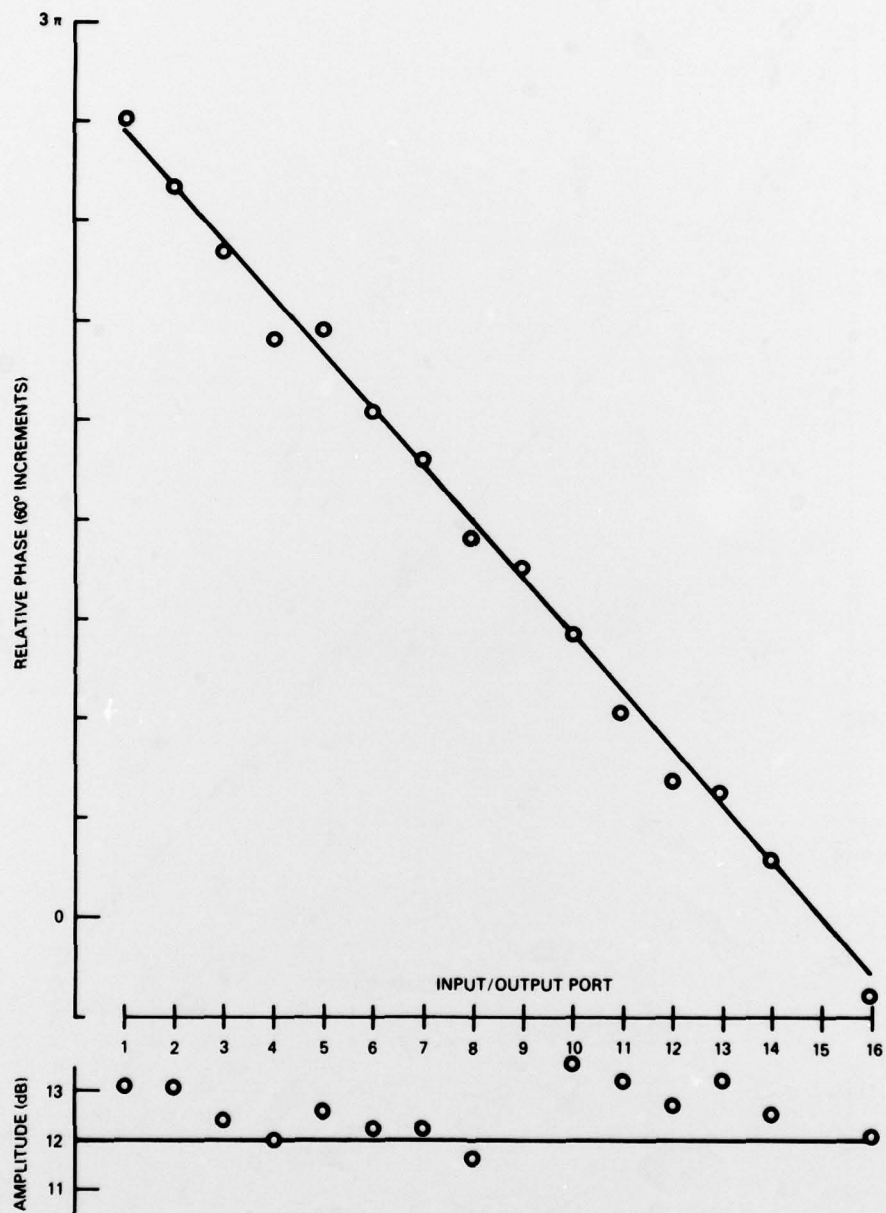


Fig. A15 — Input signal into port 15 (2L)

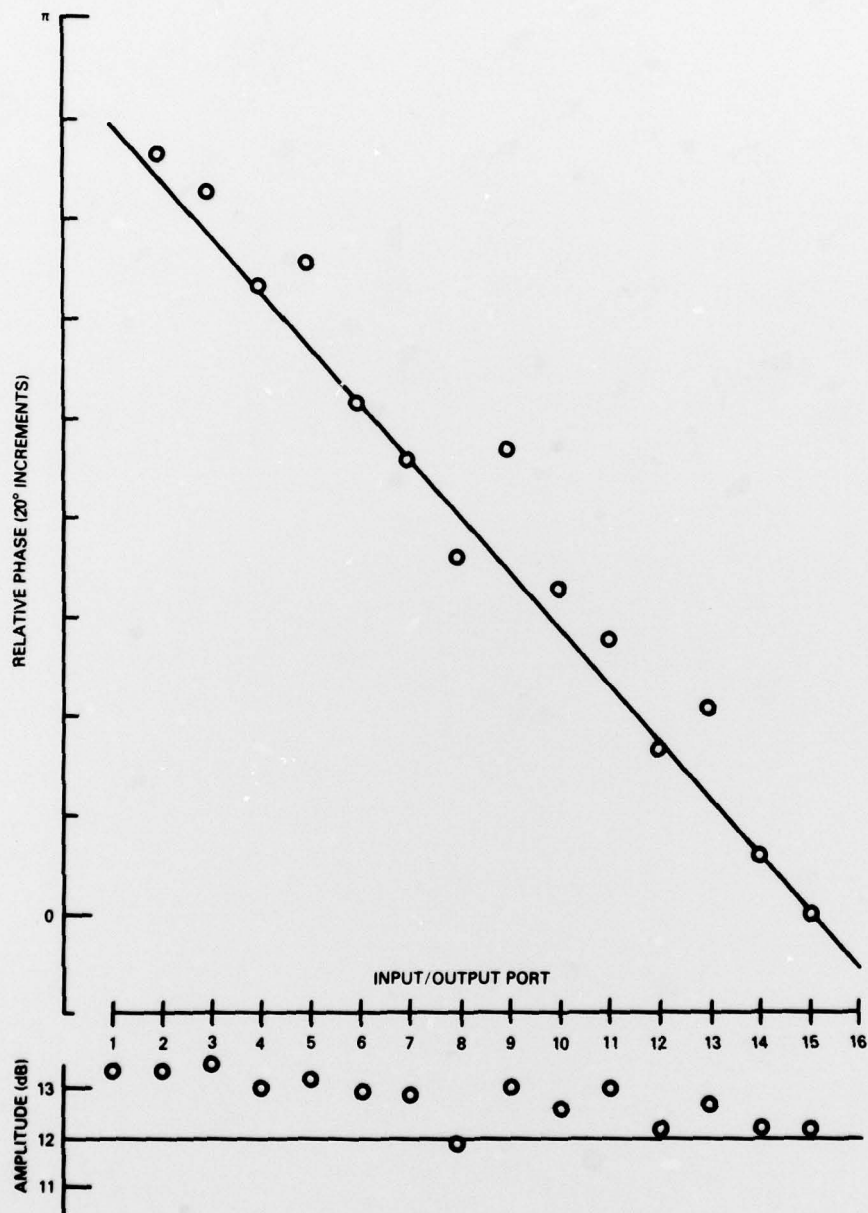


Fig. A16 — Input signal into port 16 (1L)